

Radiation pions in two-nucleon effective field theory

Thomas Mehen^x and Iain W. Stewart^y

California Institute of Technology, Pasadena, CA, USA 91125

Abstract

For interactions involving two or more nucleons it is useful to divide pions into two classes, potential and radiation. Radiation pions can be integrated out for momenta $p \ll Q_r$, where $Q_r = \sqrt{M_N m}$ is the pion production threshold. For $p \sim Q_r$ these pions need to be included, and we show that this can be done consistently with a power counting in Q_r . The leading order radiation pion graphs which contribute to NN scattering are evaluated in the PDS and OS renormalization schemes and are found to give a small contribution.

^xmehen@theory.caltech.edu
^yiaiw@theory.caltech.edu

Effective field theory is a useful method for describing two-nucleon systems [1]. Recently, Kaplan, Savage, and Wise (KSW) [2,3] introduced a power counting which accounts for the effect of large scattering lengths. A similar power counting is discussed in Ref. [4]. According to the KSW power counting, the leading order calculation involves only a dimension 6, four-nucleon operator which is treated nonperturbatively. Higher derivative operators and pion exchange are treated perturbatively.

In general, pion exchange can be separated into two types. For a pion with energy k_0 and momentum k , a potential pion has $k_0^2 = M^2$ where M is the nucleon mass, while a radiation pion has $k_0^2 = k^2 + m^2$. As the names imply, potential pions give the dominant contribution to pion exchange between two nucleons, while radiation pions include external on-shell pions. In non-relativistic theory, integrals over loop energy are performed via contour integration. Potential pions come from contributions from the residue of a nucleon pole. For these pions, the energy dependent part of the pion propagator is treated as a perturbation because the loop energy, $k_0^2 = M^2 - k^2$, where k is the loop momentum. The residues of pion propagator poles give radiation pion contributions.

In this paper, a power counting for graphs with radiation pions is given. To illustrate this power counting, we compute the leading radiation pion contribution to S-wave nucleon-nucleon scattering.

In NRQCD (NRQED) [5], graphs involving gluons (photons) are also divided into radiation and potential pieces [6,8]. The case of pions in nuclear theory is novel because pions are massive. There is a new scale associated with the threshold for pion production, which occurs at energy $E = m$ in the center of mass frame. This corresponds to a nucleon momentum $p = Q_r$, where $Q_r = \sqrt{M^2 - m^2} = 360 \text{ MeV}$. It is possible to introduce separate potential and radiation pion fields as was done for gluons in Ref. [8]. Because the radiation pion fields cannot appear as an on-shell degree of freedom below the threshold $E = m$, one expects that the radiation pion can be integrated out for $p < Q_r$. (Potential pions should be included for $p > m = 2$.) The full theory with both potential and radiation pions has operators in the Lagrangian with powers of m_q which give all the m dependence. If the radiation pions are integrated out, then the chiral expansion is no longer manifest because there will be m dependence hidden in the coefficients of operators in the Lagrangian containing only nucleon and potential pions. One is still justified in considering the same Lagrangian, but predictive power is lost since it is no longer clear that chiral symmetry relates operators with a different number of pion fields. Also, the m dependence induced by the radiation pions may affect the power counting of operators. For example, as shown in

Ref. [9], integrating out a radiation pion in the one-nucleon sector induces a nucleon electric polarizability $\propto 1/m_\pi$. Alternatively, one can keep chiral symmetry manifest by working with coefficients in the full theory and including radiation pion graphs. This is the approach we will adopt.

The presence of the scale Q_r modifies the power counting of the theory with radiation pions. In the KS power counting, one begins by taking external momenta $p \ll Q$. The theory is organized as an expansion in powers of Q . To estimate the size of a graph, loop momenta are taken to be of order Q . While this is correct for graphs with only potential pions, potential loops within graphs with radiation pions can actually be dominated by three momenta of order Q_r . To see how this comes about, consider as an example the graph shown in Fig. 1c. Let q be the momentum running through the pion propagator, and let k be the loop momentum running through a nucleon bubble inside the radiation pion loop. The poles from the pion propagator are

$$\frac{i}{q_0^2 - \vec{q}^2 - m^2 + i} = \frac{i}{(q_0 - \sqrt{\vec{q}^2 + m^2 + i})(q_0 + \sqrt{\vec{q}^2 + m^2 + i})}; \quad (1)$$

so the radiation pion has $\sqrt{\vec{q}^2 + m^2}$. This energy also goes into the nucleon bubbles. The k integrand is largest when the nucleons are close to their mass shell. But since the energy going into the loop is m , this occurs when $k^2 \approx M^2 - m^2$, i.e., $k \approx Q_r$. We will begin by considering the contribution of radiation pions to elastic nucleon scattering at the threshold, $E = m$. At this energy, external and loop momenta are of the same size and power counting is easiest. Because $p \approx Q_r$ it is obvious that we want to count powers of Q_r rather than Q .

Before discussing the power counting, recall the Lagrangian with pions and nucleons [3]:

$$\begin{aligned} \mathcal{L} = & \frac{f^2}{8} \text{Tr}(\partial_\mu \partial^\mu \Sigma) + \frac{f^2}{4} \text{Tr}(m_q + m_q^\dagger) + \frac{ig_A}{2} N^\dagger \gamma_5 (\partial_\mu \Sigma^\dagger - \Sigma \partial_\mu) N \\ & + N^\dagger i \not{D}_0 N + \frac{D^2}{2M} N^\dagger C_0^{(s)} (N^\dagger P_i^{(s)} N)^\dagger (N^\dagger P_i^{(s)} N) \\ & + \frac{C_2^{(s)} \hbar}{8} (N^\dagger P_i^{(s)} N)^\dagger (N^\dagger P_i^{(s)} \nabla^2 N) + \text{h.c.} + D_2^{(s)} \text{Tr}(m) (N^\dagger P_i^{(s)} N)^\dagger (N^\dagger P_i^{(s)} N) + \dots \end{aligned} \quad (2)$$

Here $g_A = 1.25$ is the nucleon axial-vector coupling, $\Sigma = e^{i\pi/f}$ is the exponential of pion fields, $f = 131 \text{ MeV}$ is the pion decay constant, $m = \frac{1}{2}(m_q + m_q^\dagger)$, where $m_q = \text{diag}(m_u, m_d)$ is the quark mass matrix, and $m^2 = m(m_u + m_d)$. The matrices $P_i^{(s)}$ project onto states of definite spin and isospin, and the superscript s denotes the partial wave amplitude mediated by the operator. This paper will be concerned only with S-wave scattering, so $s = {}^1S_0; {}^3S_1$.

The C_0 operator mediates S-wave nucleon transitions. The D_2 operator is important because it will be necessary to introduce counterterms proportional to m^2 to regulate UV

divergences appearing in the graphs evaluated below. The parameters appearing in Eq. (2) are bare parameters which require renormalization. For systems with two or more nucleons, it is necessary to introduce finite subtractions in order to obtain manifest power counting. Two such renormalization schemes are Power Divergence Subtraction (PDS) [2,3] and a momentum subtraction scheme (OS) [11]. These renormalization schemes are discussed extensively in Ref. [12]. The renormalized coefficient $C_0(\mu_R) = 4 = (M_R)$ where μ_R is the renormalization point. A loop with two nucleon propagators gives $M^p = (4)$, so for $\mu_R = p$ the $C_0(\mu_R)$ bubble graphs should be summed. For a scattering length a , this summation includes powers of ap to all orders [2], as desired since a is large. The coefficients $C_2(\mu_R)$ and $D_2(\mu_R)$ scale as $1 = \frac{2}{R}$, so for $\mu_R = p$ they are treated perturbatively. The ellipsis in Eq. (2) denotes higher order terms including contact interactions which for NN scattering begin to contribute at NNLO. These will not be considered here.

Next, we introduce the power counting at the scale Q_r . A scheme with manifest power counting will be used, so that that $C_0(\mu_R) = 1 = (M_R)$; $C_2(\mu_R) = 1 = (M_R^2)$, etc., where is the range of the theory. We will take $p = \mu_R = Q_r$. A radiation loop has $q_0 = q$ so $d^4q = Q_r^8 = M^4$, where q is the momentum running through the pion propagator. A radiation pion propagator gives a $M^2 = Q_r^4$, while the derivative associated with a pion-nucleon vertex gives $Q_r^2 = M$. A nucleon propagator gives a $M = Q_r^2$. External energies and momenta are kept in the nucleon propagator since $E = p^2 = M = Q_r^2 = M$. Furthermore, it is appropriate to use a multipole expansion for radiation pion-nucleon vertices which is similar to the treatment of radiation gluons in NRQCD [7]. Therefore, radiation pions will not transfer three-momenta to a nucleon. This is usually equivalent to expanding in powers of a loop momentum divided by M before doing the loop integral. A potential loop will typically have running through it an energy $Q_r^2 = M$ (either an external or radiation loop energy). Therefore, in these loops the loop energy $k_0 = Q_r^2 = M$, while the loop three momentum $k = Q_r$, so $d^4k = Q_r^5 = M$. It is not inconsistent for $k = Q_r$ while $q = Q_r^2 = M$, since three momenta are not conserved at the nucleon-radiation pion vertices. We will see through explicit examples that this power counting correctly estimates the size of radiation pion graphs.

Note that only the potential loop measure gives an odd power of Q_r , so without potential loops the power counting reduces to power counting in powers of M . The power counting here therefore correctly reproduces the usual chiral power counting used in the one nucleon sector [10]. For graphs with a single nucleon a static propagator may be used. However, for graphs with two nucleons the propagators always include the kinetic energy term. At the scale Q_r potential pion propagators may still be treated in the same way, i.e. $(k_0^2 - k^2 - m^2) =$

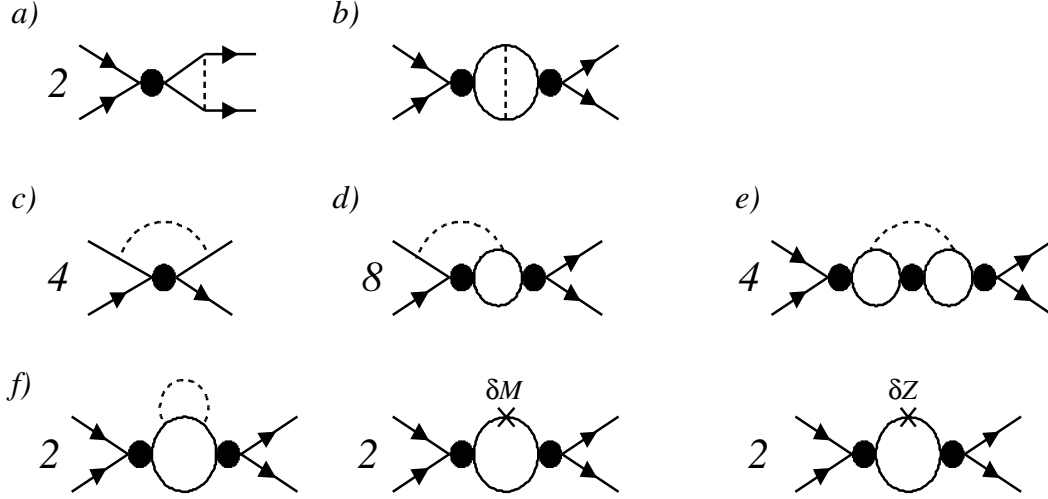


FIG. 1. Leading order radiation pion graphs for NN scattering. The solid lines are nucleons, the dashed lines are pions and M , Z are the mass and field renormalization counterterms. The filled dot denotes the $C_0(\mathbf{r})$ bubble chain. There is a further field renormalization contribution that is calculated in text, but not shown.

$i = (k^2 + m^2) + O(k_0^2 = k^4)$, which has an expansion in $Q_r^2 = M^2$.

Graphs with one radiation pion and additional higher order contact interactions or potential pions are suppressed by factors of $Q_r =$ relative to graphs with a single radiation pion and C_0 vertices. The Q_r expansion is a chiral expansion about $m = 0$, so there is a limit of QCD where it is justified. The scale is unknown. One possible estimate is $p_{NN} = 8 \sqrt{f^2(M g_A^2)} = 300 \text{ MeV}$ since a graph with $m + 1$ potential pions is suppressed by $p = 300 \text{ MeV}$ relative to a graph with m potential pions. However, this order of magnitude estimate only takes into consideration a partial subset of the graphs of the theory. As argued in Ref. [12], it is possible that the range is of order the scale of short range interactions that are integrated out, implying 500 MeV . In fact, the accuracy of NLO computations of nucleon-nucleon phase shifts is in agreement with this physically motivated estimate of the range. We will assume that an expansion in $Q_r =$ is valid. This hypothesis will be tested further by seeing how well the effective theory makes predictions at $p = 300 \text{ MeV}$. For example, processes with external pions could be considered. If the $Q_r =$ expansion is not convergent, then application of the theory is restricted to $p < Q_r$. For these momenta, radiation pions could be integrated out, and thus omitted from the calculation altogether.

The radiation pion graphs that give the leading order contribution to nucleon-nucleon scattering are shown in Fig. 1. The filled dot denotes the leading order interaction between nucleons, a $C_0(\mathbf{r})$ bubble sum. We illustrate the power counting with an example, the graph

in Fig. 1d. For the moment, replace the C_0 bubble sums with single C_0 vertices. Each C_0 gives a factor of $1/M Q_r$ and each nucleon line gives a factor $M = Q_r^2$. The derivatives from the pion couplings combine with the radiation pion propagator to give a factor of unity. The radiation loop gives $Q_r^8 = M^4$, while the nucleon bubble loop gives $Q_r^5 = M$. There is also a factor of $1=f^2$ from pion exchange, and two factors of $1=4$ from the radiation loop giving a $1=2$. (1 GeV is the chiral symmetry breaking scale.) Combining all factors, we find that this graph scales like $Q_r^3 = (M^3)^{1/2}$. This graph is suppressed relative to the leading order amplitude, $A^{(1)}$, by factor of $Q_r^4 = (M^2)^2 = m^2 = 2$. Note that C_0 bubbles are summed on external nucleon lines as well as in the interior of the radiation loop, and each graph in the sum has the same size. It is straightforward to verify that all graphs in Fig. 1 scale the same way. For external bubble sums we can simply use the vertex $iA^{(1)}$ where $A^{(1)}$ is the leading order S-wave amplitude,

$$A^{(1)} = \frac{4}{M} \frac{1}{+ip}; \quad (3)$$

and the pole $= 4 = M C_0(R) + R = 1=a$. Graphs with two radiation pions are suppressed by at least $Q_r^8 = (M^4)^2 = m^4 = 4$ and will not be considered.

The first graphs we consider are those in Fig. 1a,b. These graphs have contributions from potential and radiation pions, and it may not be obvious that a clean separation occurs. Here the energy integrals will be evaluated without any approximations, after which the graphs split into radiation and potential parts. The graph in Fig. 1a gives:

$$iA^{(1)} \frac{g_A^2}{2f^2} \int \frac{d^D q}{(2\pi)^D} \frac{i}{\frac{E}{2} + q_0} \frac{i}{q^2 - \frac{(q-p)^2}{2M} + i} \frac{i}{q^2 - \frac{(q-p)^2}{2M} + i} \frac{i q^2}{q^2 - m^2 + i}; \quad (4)$$

Throughout this paper we will include a factor of $(-2)^{4-D}$ in the loop measures. Performing the q_0 integral gives a term from the residue of the nucleon pole and a term from the pion pole,

$$iA^{(1)} \frac{g_A^2}{2f^2} \int \frac{d^n q}{(2\pi)^n} \frac{M}{(q-p)^2 - M E} \frac{q^2}{q^2 + m^2 - \frac{E}{2} - \frac{(q-p)^2}{2M}}; \quad (5)$$

$$iA^{(1)} \frac{g_A^2}{4f^2} \int \frac{d^n q}{(2\pi)^n} \frac{q^2}{q^2 + m^2 - \frac{E}{2} + \frac{(q-p)^2}{2M}} \frac{1}{q^2 + m^2 - \frac{(q-p)^2}{2M} - \frac{E}{2}} \frac{1}{q^2 + m^2 - \frac{(q-p)^2}{2M}}; \quad (6)$$

where $n = D - 1$. Eq. (5) is the potential pion contribution. Expanding in $\frac{E}{2} - \frac{(q-p)^2}{2M} = \left[\frac{2q \cdot p - q^2}{2M}\right]^2$ gives the result in Ref. [2,3], and subleading terms suppressed by $Q_r^2 = M^2$. Eq. (6) is the radiation pion contribution. With $|q| < M$, we may take $(q-p)^2 = M^2 - p^2 = M^2$ in the last two propagators, which is the same approximation that is made by performing the

multipole expansion. Finally, we use the equations of motion to set $E = p^2 = M^2 = 0$. It is important to note that we have not neglected E relative to \mathbf{q} . For $n = 3, 2$, Eq. (6) becomes

$$a) = iA^{(1)} \frac{g_A^2}{4f^2} \int \frac{d^n q}{(2\pi)^n} \frac{q^2}{(q^2 + m^2)^{3/2}} = 3iA^{(1)} \frac{g_A^2 m^2}{(4\pi f)^2} \left[\frac{1}{-2} + \frac{1}{3} \ln \frac{m^2}{-2} \right]; \quad (7)$$

where $-2 = -2e^{-E}$. Note that this integral is finite in three dimensions ($n = 2$).

The next graph we consider is shown in Fig. 1b. We have chosen to route loop momenta so that q runs through the pion and k and $(k+q)$ run through the nucleon lines. The momentum k is potential, while q can be potential or radiation. Doing the k_0 contour integral and combining the two terms gives:

$$2iA^{(1)} \int \frac{g_A^2}{2f^2} \frac{d^n k}{(2\pi)^n} \frac{d^D q}{(2\pi)^D} \frac{q^2}{q_0^2} \frac{q^2}{q^2 + m^2 + i\epsilon} \frac{1}{E \frac{k^2}{M} + i\epsilon} \frac{1}{E \frac{(k+q)^2}{M} + i\epsilon} \quad (8)$$

$$\frac{E \frac{(k+q)^2}{2M} \frac{k^2}{2M}}{E \frac{(k+q)^2}{2M} \frac{k^2}{2M} q + i\epsilon} \frac{E \frac{(k+q)^2}{2M} \frac{k^2}{2M}}{E \frac{(k+q)^2}{2M} \frac{k^2}{2M} + q_0 + i\epsilon} :$$

Doing the q_0 integral gives two terms, but the radiation and potential contributions are still mixed. Combining these gives

$$iA^{(1)} \int \frac{g_A^2}{2f^2} \frac{d^n k d^n q}{(2\pi)^{2n}} \frac{q^2}{q^2 + m^2} \frac{1}{E \frac{k^2}{M}} \frac{1}{E \frac{(k+q)^2}{M}} \frac{1}{E \frac{(k+q)^2}{2M} \frac{k^2}{2M}} \frac{1}{q^2 + m^2}; \quad (9)$$

which can be split into potential and radiation parts

$$iA^{(1)} \int \frac{g_A^2}{2f^2} \frac{d^n k}{(2\pi)^n} \frac{d^n q}{(2\pi)^n} \frac{q^2}{q^2 + m^2} \frac{1}{E \frac{k^2}{M}} \frac{1}{q^2 + m^2} \frac{1}{\frac{(2k \cdot q + q^2)}{2M}} \quad (10)$$

$$+ \frac{1}{E \frac{(k+q)^2}{M}} + \frac{1}{E \frac{k^2}{M} \frac{(2k \cdot q + q^2)}{2M}} \frac{1}{q^2 + m^2} :$$

The first term in Eq. (10) is the two-loop potential pion graph evaluated in Ref. [3]. The factors of $(2k \cdot q + q^2) = (2M^2)$ appearing in the denominators can be dropped because the loop integral is dominated by $k, q \ll M$ and therefore $(2k \cdot q + q^2) = (2M^2) \frac{q^2}{q^2 + m^2}$. For the second term, which is the radiation pion contribution, this is equivalent to the multipole expansion. Momenta $k \ll M$ and $q \ll m$ dominate the integrals in the second term. In Ref. [13], the potential and radiation parts of the graph in Fig. 1b were evaluated in the limit $m = 0$, and shown to correctly make up the corresponding part of the fully relativistic calculation. The calculation in Ref. [13] agrees with Eq. (10) for $m = 0$. Note that the

radiation part would not agree if we assumed $k = m$ and used static nucleon propagators in the radiation loop¹. For $n = 3$ the radiation part of Eq. (10) is

$$\begin{aligned} b) &= iA^{(1)} \int \frac{g_A^2}{2f^2} \frac{d^n k}{(2\pi)^n} \frac{d^n q}{(2\pi)^n} \frac{q^2}{q^2 + m^2} \frac{1}{E - \frac{k^2}{M}} \frac{1}{E - \frac{k^2}{M}} \frac{1}{q^2 + m^2} \\ &= A^{(1)} \int \frac{g_A^2 M m^2}{(4\pi f)^2} \left(\frac{3p}{4} \frac{1}{-} + \frac{7}{3} \frac{1}{2} \ln 2 - \ln \frac{m^2}{-2} - \ln \frac{p^2}{-2} + \frac{i}{4} \frac{p}{M m} I_1 \frac{E}{m} \right); \end{aligned} \quad (11)$$

where

$$I_1(x) = \frac{3}{2} \frac{(\frac{5}{4})}{(\frac{5}{4})} {}_3F_2 \left(\frac{5}{4}; \frac{1}{4}; \frac{1}{4}; g; f; \frac{1}{2}; \frac{5}{4}; g; x^2 \right) + \frac{x (\frac{1}{4})}{(\frac{1}{4})} {}_3F_2 \left(\frac{3}{4}; \frac{1}{4}; \frac{3}{4}; g; f; \frac{3}{2}; \frac{7}{4}; g; x^2 \right); \quad (12)$$

For $n = 2$ the loop integral in Eq. (11) is finite. Since $A^{(1)} = 1/(M - Q_r)$ the results in Eqs. (7, 11) are order $Q_r^3/(M^3 - 2)$ as expected. At one-loop the $1=$ pole in Eq. (7) is cancelled by a counterterm²

$${}^{uv,1a}D_2 = -3C_0^{\text{nite}} \frac{g_A^2}{(4\pi f)^2} \frac{1}{-} E + \ln(-); \quad (13)$$

For higher loops the $1=$ poles in Eq. (7), Eq. (11), and ${}^{uv,1a}D_2$ dressed with C_0 bubbles cancel. Note that the $O(-)$ piece of the bubbles give a finite contribution,

$$C_0(-) = \frac{M p}{4} \left(1 + \frac{1}{2} \frac{1}{2} \ln 2 - \ln \frac{p^2}{-2} - \frac{i}{4} \frac{p}{M m} \right); \quad (14)$$

The result of combining Figs. 1a,b and ${}^{uv,1a}D_2$ dressed by C_0 bubbles is:

$$a) + b) = 3iA^{(1)} \int \frac{g_A^2 m^2}{(4\pi f)^2} \frac{M}{4} \frac{1}{3} \ln \frac{m^2}{-2} + iA^{(1)} \int \frac{g_A^2 M m^2}{(4\pi f)^2} \frac{p}{4} \frac{M m}{-} I_1 \frac{E}{m}; \quad (15)$$

Next we consider the graphs in Fig. 1c,d,e. The loop integrals in these graphs vanish if the pion pole is not taken so there is no potential pion contribution. As pointed out in Ref. [3], emission of the radiation pion in these graphs changes the spin/isospin of the nucleon pair. Therefore, if the external nucleons are in a spin-triplet (singlet) state, then the coefficients appearing in the internal bubble sum are $C_0^{(1S_0)}(-)$ ($C_0^{(3S_1)}(-)$). The notation C_0 (C_0^0) will be used for vertices outside (inside) the radiation pion loop. We begin with

¹Furthermore, if static nucleon propagators are used one obtains a linear divergence requiring a non-analytic counterterm $\propto 1/m$ [14].

²The bare coefficients are written as $C^{\text{bare}} = {}^{uv}C_P + C^{\text{nite}}$. In OS and PDS additional finite subtractions are made so that $C^{\text{nite}} = C(-) - {}^nC(-)$, see Ref. [12].

Fig. 1c. The contribution from the graph with m nucleon bubbles in the internal bubble sum is

$$i \frac{g_A^2}{2f^2} \int \frac{d^D q}{(2\pi)^D} \frac{i}{q_0} \frac{i}{q_0} \frac{i q^2}{q^2} \frac{1}{m^2 + i} [i C_0^0(\mathbf{R})]^{m+1} \int \frac{d^D k}{(2\pi)^D} \frac{i}{k_0} \frac{i}{q + \frac{E}{2}} \frac{i}{\frac{(k+q)^2}{2M} + i} \frac{i}{k_0 + \frac{E}{2}} \frac{i}{\frac{k^2}{2M} + i} ; \quad (16)$$

where we used the multipole expansion and then the equations of motion to eliminate E and p from the first two propagators. All nucleon propagators have a q pole above the real axis, while the pion propagator has one pole above and one below. Therefore, the q_0 contour is closed below. The $d^D k$ integrals are also easily performed giving

$$i \frac{g_A^2 C_0^0(\mathbf{R})}{f^2} \frac{C_0^0(\mathbf{R}) M}{(4\pi)^{n=2}} \frac{(1-n=2)^{m+1}}{(2\pi)^n} \frac{d^n q}{(2\pi)^n} \frac{q^2}{(q^2 + m^2)^{3=2}} \frac{1}{(p^2 + M^2)^{n=2-1}} \frac{i_m}{R} ; \quad (17)$$

Note the size of the momentum running through the nucleon bubbles is set not by the external momentum p but rather by $\frac{p}{M}$. The R inside the parenthesis comes from inclusion of the PDS or OS $C_0^0(\mathbf{R})$ counterterm graphs for the internal bubble sum. The integral will be dominated by $q \sim m$ so the graph will scale as

$$\frac{1}{2} \frac{m^2}{M R} \frac{p}{M m} \frac{1}{R} ; \quad (18)$$

Since $R \sim \frac{p}{M m}$, all graphs in the sum are of order $Q_F^3 = (M^{-3-2})$.

For Figs. 1c,d,e the sum over bubbles should be done before the radiation loop integral. The reason is that an arbitrary term in the bubble sum has a much different dependence on the energy flowing through it than the sum itself. This can be seen in the q dependence in Eq. (17). If we integrate over q then terms in the sum may diverge whereas the integral of the complete sum is finite. In fact, for $n = 3$, Eq. (17) has divergences of the form $(1-m=4)F(\frac{E}{m^2})$ and $(1=2-m=4)E F(\frac{E}{m^2})$ where F is a hypergeometric function. These divergences are misleading because they appear already for momenta $> 1=a$ where we know the correct form of the leading order amplitude falls off as $1=p$. For this reason the summation is performed before introducing counterterms to subtract divergences (this approach is also taken in the analysis of three body interactions in Ref. [15]). Summing over m , Eq. (17) becomes:

$$c) = i \frac{g_A^2}{f^2 M} \int \frac{d^n q}{(2\pi)^n} \frac{q^2}{(q^2 + m^2)^{3=2}} \frac{1}{p^2 + M^2} \frac{1}{q^2 + m^2} \frac{1}{(n=2-1)}$$

$$= \frac{ig_A^2}{p^2 f^2} \frac{m}{M} \stackrel{3=2}{I_2} \frac{E}{m} ;$$

where $0 = 4 - M C_0^0(\mu_R) + \mu_R \ln 1 = a$. As expected the graph scales as Q_r^3 . In the limit $n \rightarrow 3$, I_2 is finite and given by

$$I_2(x) = \frac{\left(\frac{3}{4}\right)}{\left(\frac{p}{4}\right)} {}_3F_2 \left[\begin{matrix} \frac{3}{4}; \frac{1}{4}; \frac{3}{4} \end{matrix} ; -g; \frac{1}{2}; \frac{7}{4}; g; x^2 \right] - \frac{3x}{2} \frac{\left(\frac{p}{4}\right)}{\left(\frac{p}{4}\right)} {}_3F_2 \left[\begin{matrix} \frac{1}{4}; \frac{3}{4}; \frac{5}{4} \end{matrix} ; -g; \frac{3}{2}; \frac{9}{4}; g; x^2 \right] + O\left(\frac{1}{M m}\right) : \quad (19)$$

I_2 is manifestly μ_R independent and is also finite as $n \rightarrow 2$.

Next we consider the graph in Fig. 1d. Integrals are done in the same manner as that of Fig. 1c. For $n = 3 \rightarrow 2$, Fig. 1d is

$$\begin{aligned} d) &= 4iA^{(1)} \frac{g_A^2}{2f^2} \frac{(n=2 \rightarrow 1)^2}{(4 - f)^{n=2 \rightarrow 1}} \frac{d^n q}{(2 - f)^n} \frac{q^2}{(q^2 + m^2)^{3=2}} \frac{p^2 + M^2}{p^2 + M^2} \frac{q^{n=2 \rightarrow 1}}{q^2 + m^2} \frac{(p)^{n=2 \rightarrow 1}}{(p)^{n=2 \rightarrow 1}} \\ &= 12iA^{(1)} \frac{g_A^2 m^2}{(4 - f)^2} \left[\frac{1}{-2} + \frac{1}{3} \ln \frac{m^2}{-2} \right] - 4 \frac{(p - i^0) M A^{(1)}}{4} \frac{g_A^2}{2f^2} \frac{m}{M} \stackrel{3=2}{I_2} \frac{E}{m} : \quad (20) \end{aligned}$$

Fig. 1d is finite for $n = 2$. The $1 =$ pole in Eq. (20) is cancelled by a new tree level counterterm $i^{uv;ld} D_2 m^2$ where $^{uv;ld} D_2$ has the same form as Eq. (13) except with a 12 instead of a 3 .

Evaluation of Fig. 1e is also similar to Fig. 1c. For $n = 3 \rightarrow 2$ we find:

$$\begin{aligned} e) &= 2i \frac{(p - i^0)^2}{p^2} \frac{M A^{(1)}}{4} \frac{g_A^2}{2f^2} \frac{m}{M} \stackrel{3=2}{I_2} \frac{E}{m} + iA^{(1)} \int \frac{g_A^2 M m^2}{(4 - f)^2} \frac{p}{2} \frac{M m^2}{p^2} I_1 \frac{E}{m} \\ &\quad + 12A^{(1)} \int \frac{M p}{4} \frac{g_A^2 m^2}{(4 - f)^2} \left[\frac{1}{-2} + \frac{7}{3} \ln 2 - \ln \frac{m^2}{-2} - \ln \frac{p^2}{-2} \right] \\ &\quad - 6iA^{(1)} \int \frac{M}{4} \frac{g_A^2 m^2}{(4 - f)^2} \left[\frac{1}{-2} + \frac{1}{3} \ln \frac{m^2}{-2} \right] : \quad (21) \end{aligned}$$

This graph is finite for $n = 2$. A D_2 counterterm cancels the divergence in the last line,

$$^{uv;ld} D_2 = 6 (C_0^{nite})^2 \frac{M}{4} \frac{g_A^2}{(4 - f)^2} \frac{1}{-2} E + \ln(\dots) : \quad (22)$$

For two and higher loops the remaining $1 =$ poles cancel between Eqs. (20, 21, 22) and $^{uv;ld} D_2$ dressed with C_0 bubbles, so no new counterterms need to be introduced. The $O(1)$ piece of the bubbles again give a finite contribution. Combining Figs. 1c, d, e, and $^{uv;ld} D_2$ and $^{uv;ld} D_2$ dressed with C_0 bubbles gives

$$c) + d) + e) = 2i\mathbb{A}^{(1)} \int \frac{g_A^2}{(4-f)^2} \left(6m^2 \frac{M}{4} \left(\frac{0=2}{1} \right) \frac{1}{3} \ln \frac{m^2}{2} + \frac{M^{3=2} m^{5=2}}{4} I_1 \frac{E}{m} \right. \\ \left. + \frac{(0)^2}{2} \frac{(M m)^{3=2}}{M} I_2 \frac{E}{m} \right) : \quad (23)$$

Fig. 1f shows a two loop graph with a nucleon self energy on an internal line. It is important to also include graphs with the one-loop wavefunction and mass renormalization counterterms, Z ; M inserted on the internal nucleon line. We will use an on-shell renormalization scheme for defining these counterterms, which ensures that the mass, M , appearing in all expressions is the physical nucleon mass. The counterterms are:

$$M = \frac{3g_A^2 m^3}{16 f^2} ; \quad Z = \frac{9 g_A^2 m^2}{2 (4-f)^2} \left(\frac{1}{4} + \frac{1}{3} \ln \frac{m^2}{2} \right) : \quad (24)$$

The result from the graphs in Fig. 1f is then

$$f) = -3i\mathbb{A}^{(1)} \int \frac{g_A^2}{(4-f)^2} \frac{M^{3=2} m^{5=2}}{4} I_1 \frac{E}{m} : \quad (25)$$

When Eq. (25) is added to Eqs. (15,23) the terms proportional to I_1 cancel. To implement PDS we must consider the value of the graphs in Fig. 1f using Minimal Subtraction with $n = 2$. For $n = 2+$ we have $M = 3g_A^2 m^2 / (16 f^2)$ and $Z = 0$, which makes the sum of graphs in Fig. 1f finite. Finally, renormalization of the bare nucleon fields in the Lagrangian, $N^{\text{bare}} = \sqrt{Z} N$, $Z = 1 + Z$, induces a four-nucleon term

$$L = C_0^{(s); \text{nite}} (2 - Z) (N^T P_i^{(s)} N)^Y (N^T P_i^{(s)} N) : \quad (26)$$

Since $Z = Q^4 / Q^2$ this term is treated perturbatively. A tree level counterterm

$${}^{uv,0}D_2 = 9C_0^{\text{nite}} \frac{g_A^2}{(4-f)^2} \frac{h_1}{2} E + \ln(\)^i \quad (27)$$

is introduced to cancel the $1=$ pole. Dressing the operator in Eq. (26) with C_0 bubbles gives

$$9i\mathbb{A}^{(1)} \int \frac{M}{4} \frac{g_A^2 m^2}{(4-f)^2} \left(\frac{1}{3} + \ln \frac{2}{m^2} \right) : \quad (28)$$

Again, for $n = 2$ we have $Z = 0$ so no new PDS counterterms were added. Note that if we had instead used bare nucleon fields then there would be no correction of the form in Eq. (26). However, Eq. (25) would be modified because the last graph in Fig. 1f is no longer present. When this is combined with the contribution from the LSZ formula the sum of Eq. (25) and Eq. (28) is reproduced.

For PDS, the graphs in Figs.1a-f are finite for $n = 2$ so no new finite subtractions were introduced. With $n = 3$ counterterms are introduced to renormalize the terms with $\ln(\mu^2)$ in Eqs. (15,23,28) (in PDS $\mu = \mu_R$). In OS only terms analytic in m^2 are subtracted [12] (including $m^2 \ln(\mu^2)$). We find $D_2(\mu_R) = D_2(\mu_R) + \delta D_2(\mu_R)$, with

$$D_2(\mu_R) = 6C_0(\mu_R)^2 \frac{g_A^2}{(4f)^2} \frac{M(\mu_R^0)}{4} \left(\frac{1}{3} + \ln \frac{\mu_R^2}{0} \right) : \quad (29)$$

Here $\mu = 1=3$ in PDS and $\mu = 0$ in OS, and μ_0 is an unknown scale. Note that the logarithm in Eq. (29) gives a contribution to the beta function for $D_2(\mu_R)$ of the form

$$\beta_{D_2}^{(\text{rad})} = \frac{3g_A^2}{4f^2} \frac{M(\mu_R^0)}{4} C_0(\mu_R)^2 : \quad (30)$$

This disagrees with the beta function of Ref. [3], because in that paper the beta function was calculated including only the one-loop graphs.

Adding the contributions in Eqs. (15,23,25,28) gives the total radiation pion contribution to the amplitude at order Q_r^3 :

$$\begin{aligned} iA^{\text{rad}} = & 6iA^{(1)} \int \frac{g_A^2 m^2}{(4f)^2} \frac{M(\mu_R^0)}{4} + \ln \frac{\mu_R^2}{m^2} iA^{(1)} \int \frac{D_2(\mu_R) m^2}{C_0(\mu_R)^2} \\ & + iA^{(1)} \int \frac{M(\mu_R^0)}{4} \frac{g_A^2}{f^2} \frac{m}{M} {}^3I_2 \frac{E}{m} : \end{aligned} \quad (31)$$

The first term here has the same dependence on the external momentum as an insertion of the D_2 operator dressed by C_0 bubbles. Its μ_R dependence is cancelled by μ_R dependence in $D_2(\mu_R)$. Note that due to cancellations between graphs, this term is actually suppressed by a factor of μ_R relative to what one expects from the power counting. The second term in Eq. (31) has a nontrivial dependence on E and is suppressed by an even smaller factor of $\mu_R^2 = Q_r^2$. These cancellations were not anticipated by the power counting and it would be interesting to determine if the suppression by factors of $\mu_R = a$ continues at higher orders. If so, this might be a consequence of an additional symmetry of the theory in the limit $a \rightarrow 1$. If not, terms at order Q_r^4 may actually give the leading contribution of radiation pions to NN scattering.

If we now consider momenta $p = m + Q = Q_r$, we should μ_R at the threshold, $\mu_R = \mu_0$, and expand in $E = m$ giving $I_2(E = m) = 3.94 + O(E = m)$. Therefore, the dominant effect of the graphs that occur at order Q_r^3 is indistinguishable from a shift in $D_2(\mu_R)$. Integrating out the radiation pions amounts to absorbing their effects into the effective D_2 in the theory with only potential pions. The result in Eq. (31) is suppressed



FIG. 2. Example of order Q_r^4 radiation pion graphs for NN scattering.

relative to the NLO contributions in Ref. [3] by a factor of roughly $2(M_\pi/m)^4 = 10$. Since this is smaller than the expansion parameter, $Q_r = 1/3$, it can be neglected at NNLO.

At order Q_r^4 graphs such as those in Fig. 2 will contribute to NN scattering. The graph in Fig. 2a includes an insertion of the operator

$$L = iG_2^{(s)} \bar{N}^T P_i^{(s)} N \bar{N}^T P_i^{(s)} N (\partial_j^\mu \partial_j^\mu N) + \text{h.c.} \quad (32)$$

This graph will be dressed with C_0 bubbles inside and outside the radiation pion loop. The renormalization group equation for G_2 gives $G_2(R) = 1/(M_R^2) = 1/(M^2 Q_r^2)$. Combining this with the remaining factors of Q_r we find that Fig. 2a is of order $Q_r^4 = (M^4/m^2)$ and is therefore suppressed by $Q_r = M$ relative to a graph in Fig. 1. Power counting the graph in Fig. 2b gives $Q_r^4 = (M^3/m^2)$, giving a factor of $Q_r = M$ relative to a graph in Fig. 1. This provides an example of how graphs with potential pions seem to restrict the range of the effective field theory to $m_{NN} \approx 300 \text{ MeV}$. The 300 MeV scale applies only to a subset of graphs and may change once all graphs at this order are included.

To summarize, we have introduced a power counting in factors of $Q_r = \frac{p}{M m}$ appropriate for graphs with radiation pions. The order Q_r^3 contributions to NN scattering were computed and found to be suppressed by inverse powers of the scattering length. Higher order corrections are suppressed by factors of Q_r and whether or not this expansion is convergent is an open question. If the range of the two-nucleon effective field theory with perturbative pions is really 300 MeV, and the suppression by factors of Q_r does not persist at higher orders then contributions from radiation pions induce an uncalculable error of order $m^2 = 2$ to the NN scattering amplitude in this theory. The validity of the $Q_r = M$ expansion can be tested by looking at processes at $p \approx 300 \text{ MeV}$ such as those with external pions.

We would like to thank Mike Luke and Mark Wise for several enlightening discussions, as well as S. Fleming, D. B. Kaplan and U. van Kolck for their comments. This work was supported in part by the Department of Energy under grant number DE-FG 03-92-ER 40701. T.M. was also supported by a John A. McCone Fellowship.

REFERENCES

- [1] S. Weinberg, Phys. Lett. B 251 (1990) 288; Nucl. Phys. B 363 (1991) 3; C. Ordóñez and U. van Kolck, Phys. Lett. B 291 (1992) 459; C. Ordóñez, L. Ray and U. van Kolck, Phys. Rev. Lett. 72 (1994) 1982; Phys. Rev. C 53 (1996) 2086; U. van Kolck, Phys. Rev. C 49 (1994) 2932. G. P. Lepage, nucl-th/9706029. D. B. Kaplan, M. J. Savage, and M. B. Wise, Nucl. Phys. B 478 (1996) 629.
- [2] D. B. Kaplan, M. J. Savage, and M. B. Wise, Phys. Lett. B 424 (1998) 390.
- [3] D. B. Kaplan, M. J. Savage, and M. B. Wise, Nucl. Phys. B 534 (1998) 329.
- [4] U. van Kolck, hep-ph/9711222 and nucl-th/9808007.
- [5] W. E. Caswell and G. P. Lepage, Phys. Lett. B 167 (1986) 437; G. T. Bodwin, E. Braaten, and G. P. Lepage, Phys. Rev. D 55 (1997) 1125.
- [6] M. Luke and A. Manohar, Phys. Rev. D 55 (1997) 4129; P. Labelle, Phys. Rev. D 58 (1998) 093013.
- [7] B. Grinstein and I. Rothstein, Phys. Rev. D 57 (1998) 78.
- [8] M. Luke and M. J. Savage, Phys. Rev. D 57 (1998) 413.
- [9] V. Bernard, N. Kaiser, and U. Meißner, Phys. Rev. Lett. 67, 1515 (1991); Nucl. Phys. B 373, 364 (1992); Phys. Lett. B 319, 269 (1993).
- [10] E. Jenkins and A. Manohar, Phys. Lett. B 255 (1991) 558, *ibid* B 259 (1991) 353.
- [11] J. Gegelia, nucl-th/9802038; T. Mehen, and I. Stewart, nucl-th/9809071.
- [12] T. Mehen and I. Stewart, hep-ph/9809095.
- [13] M. Beneke and V. A. Smirnov, Nucl. Phys. B 522 (1998) 321.
- [14] N. Shore and G. Rupak, private communication.
- [15] P. F. Bedaque and U. van Kolck, Phys. Lett. B 428 (1998) 221; P. F. Bedaque, H. W. Hammer, and U. van Kolck, Phys. Rev. C 58 (1998) R641.